Transport anomalies due to anisotropic interband scattering

Maxim Breitkreiz, P. M. R. Brydon, and Carsten Timm[*]

Institute of Theoretical Physics, Technische Universität Dresden, 01062 Dresden, Germany
(Received 10 May 2013; revised manuscript received 12 July 2013; published 2 August 2013)

Unexpected transport behavior can arise due to anisotropic single-particle scattering in multiband systems. Specifically, we show within a semiclassical Boltzmann approach beyond the relaxation-time approximation that anisotropic scattering between electronlike and holelike Fermi surfaces generically leads to negative transport times, which in turn cause negative magnetoresistance, an extremum in the Hall coefficient, and a reduction of the resistivity. The anisotropy required for this to occur decreases with increasing mismatch between the Fermi-surface radii.

I. INTRODUCTION

In basic transport theory, the acceleration of carriers by an applied electric field is balanced by scattering, leading to a steady state with constant drift current.[1] The direction of the drift current is determined by the charge of the carriers and relaxes over a characteristic transport time (TT). Deviations from this basic picture tend to generate a lot of interest. A striking example are *negative* TTs: Some fraction of the carriers may drift in the direction opposite of what one would expect based on their charge. Negative TTs of minority carriers were predicted for systems with electron- and holelike Fermi surfaces (FSs),[2] based on strong electron-hole (two-particle) scattering. This *carrier drag* was first observed in semiconductor quantum wells.[3]

In this paper, we explore a different origin of negative TTs and its consequences for transport: Negative TTs can also arise due to anisotropic single-particle scattering[4] in multiband systems. In the case of *isotropic* scattering, the TTs are equivalent to the usual quasiparticle lifetimes. Anisotropic scattering, on the other hand, favors certain scattering angles. As a result, the transport coefficients can deviate significantly from the expectation based on the bare lifetimes.

Anisotropic single-particle scattering in multiband systems can be realized in materials close to an excitonic instability, e.g., electron-hole bilayers,[5] the iron pnictides,[6–8] chromium and its alloys,[9,10] and the transition-metal dichalcogenides.[11,12] In these materials, nesting of electron and hole FSs strongly enhances interband spin or charge fluctuations with a wave vector close to the nesting vector **Q**. These fluctuations are expected to promote highly anisotropic scattering between the nested FSs.

In the iron pnictides, the effect of such scattering seems to be especially pronounced, as the normal-state transport coefficients show highly anomalous behavior. In particular, the unexpectedly small magnetoresistance is hard to reconcile with the strongly enhanced Hall coefficient if analyzed based on a simple multiband model with *positive* transport times.[13] In these materials, anisotropic scattering is thought to be mainly due to spin fluctuations.[14–17] Fanfarillo *et al.*[17] have demonstrated that vertex corrections can lead to an enhancement of the Hall coefficient, which could explain its pronounced temperature dependence in the pnictides.[18,19] Vertex corrections result from the anisotropy of the scattering and are responsible for the difference between bare lifetimes

and TTs. They also show that the enhancement of the Hall coefficient is connected to negative TTs of minority carriers.[17]

In the present work we focus on the effect of anisotropic interband scattering on transport coefficients. Working within a Boltzmann approach beyond the relaxation-time approximation, we consider two FSs and include an interband scattering rate with arbitrary dependence on the scattering angle. We show that, if one FS is electronlike and the other holelike, anisotropy not only leads to an enhancement of the Hall coefficient[17] but also to an extremum. Moreover, we find a reduction of the resistivity and negative magnetoresistance as direct consequences of negative TTs.

II. MODEL AND METHOD

We consider two-dimensional (2D) and three-dimensional (3D) metals with two isotropic FSs labeled by $s = 1,2$. The center of one FS is displaced with respect to the other by a wave vector **Q** [see Fig. 1(a)]. One of the FSs may be electronlike and the other holelike (the e-h case) or both may be of the same type (the e-e or h-h case). We employ a semiclassical description in terms of the distribution function $f_{s,\mathbf{k}} = f_0(\varepsilon_{s,\mathbf{k}}) + g_{s,\mathbf{k}}$, with the equilibrium Fermi-Dirac distribution $f_0(\varepsilon_{s,\mathbf{k}})$, where $\varepsilon_{s,\mathbf{k}}$ is the band energy, and a deviation $g_{s,\mathbf{k}}$. In a weak uniform electric field **E**, the stationary state is described by the linearized Boltzmann equation:[1]

$$e\mathbf{E} \cdot \mathbf{v}_{s,\mathbf{k}}[-f_0'(\varepsilon_{s,\mathbf{k}})] = \sum_{s',\mathbf{k}'} W_{s,\mathbf{k}}^{s',\mathbf{k}'} (g_{s,\mathbf{k}} - g_{s',\mathbf{k}'}), \quad (1)$$

where $\mathbf{v}_{s,\mathbf{k}} = \hbar^{-1}\nabla_{\mathbf{k}}\varepsilon_{s,\mathbf{k}}$ is the velocity, and $W_{s,\mathbf{k}}^{s',\mathbf{k}'}$ is the scattering rate from state $s,\mathbf{k}$ to state $s',\mathbf{k}'$. The scattering term contains an in-scattering contribution proportional to $g_{s',\mathbf{k}'}$, which is equivalent to vertex corrections.

Specifically, we consider elastic scattering with an isotropic intraband contribution W_i and an in general anisotropic interband contribution $W_a(\theta_{\mathbf{k},\mathbf{k}'})$:

$$W_{s,\mathbf{k}}^{s',\mathbf{k}'} = \delta(\varepsilon_{s',\mathbf{k}'} - \varepsilon_{s,\mathbf{k}})[\delta_{s'\bar{s}} W_a(\theta_{\mathbf{k},\mathbf{k}'}) + \delta_{s's} W_i], \quad (2)$$

where $\bar{s} = 2$ (1) for $s = 1$ (2). The interband scattering rate W_a in general depends on **k** and **k**′. Since we consider a weak electric field **E**, we assume the displacements of the Fermi seas to be small compared to the Fermi momenta $k_{F,s}$. Then the range of relevant absolute values |**k**|, |**k**′| is small compared to the range of relevant polar angles, and we can ignore the
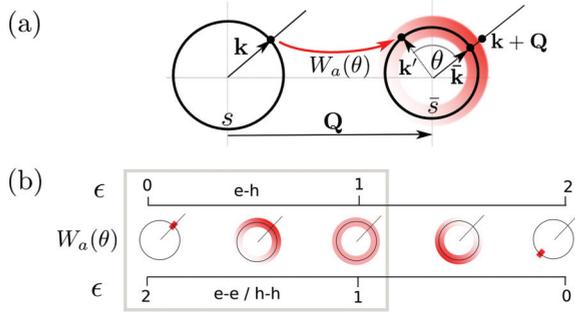
FIG. 1. (Color online) (a) Sketch of the two isotropic FSs s and $\bar{s}$, displaced by $\mathbf{Q}$, and the elastic interband scattering rate $W_a(\theta)$ (red/gray gradient). (b) Illustration of the relation between the anisotropy parameter ϵ and the shape of the function $W_a(\theta)$, for the case of $W_a(\theta)$ having a single peak. We focus on the situation in which the peak appears at $\theta = 0$, highlighted by the box.

dependence of W_a on the former. By symmetry, W_a can then only depend on the angle $\theta \equiv \theta_{\mathbf{k},\mathbf{k}'}$ spanned by $\mathbf{k}$ and $\mathbf{k}'$ [see Fig. 1(a)] and is an even function of θ.

The deviations $g_{s,\mathbf{k}}$ solving the Boltzmann equation (1) are linear in $\mathbf{E}$ and can thus be written as $g_{s,\mathbf{k}} = e\mathbf{E} \cdot \boldsymbol{\Lambda}_{s,\mathbf{k}}[-f_0'(\varepsilon_{s,\mathbf{k}})]$. Since the scattering rate $W_{s,\mathbf{k}}^{s',\mathbf{k}'}$ is an even function of θ, the scattering does not break rotational symmetry and does not introduce a preferred direction of rotation. Therefore, $\boldsymbol{\Lambda}_{s,\mathbf{k}}$ must be parallel to the only vector appearing in the equation, namely, the velocity $\mathbf{v}_{s,\mathbf{k}}$. Due to rotational symmetry, the prefactor cannot depend on $\mathbf{k}$. Thus we can write

$$g_{s,\mathbf{k}} = \tau_s e\mathbf{E} \cdot \mathbf{v}_{s,\mathbf{k}}[-f_0'(\varepsilon_{s,\mathbf{k}})], \qquad (3)$$

where τ_s is the TT for FS s, to be determined below.

Inserting Eq. (2) and performing the energy integration we obtain for the right-hand side of Eq. (1)

$$\sum_{s'} N_{s'} \langle [\delta_{s'\bar{s}} W_a(\theta) + \delta_{s's} W_i](g_{s,\mathbf{k}} - g_{s',\mathbf{k}'}) \rangle_\theta, \qquad (4)$$

where N_s is the density of states for FS s and the average over θ is denoted by $\langle \cdots \rangle_\theta = \frac{1}{\pi} \int d\theta \ldots$ for two dimensions and $\langle \cdots \rangle_\theta = \frac{1}{2} \int d\theta \sin\theta \ldots$ for three dimensions. Equation (3) shows that $g_{s',\mathbf{k}'}$ depends on θ through the velocity, which for isotropic FSs can be written as

$$\mathbf{v}_{s',\mathbf{k}'} = \eta_{s,s'} v_{F,s'} \left(\frac{\mathbf{v}_{s,\mathbf{k}}}{v_{F,s}} \cos\theta + \mathbf{e}_\perp \sin\theta \right), \qquad (5)$$

where $v_{F,s} > 0$ is the Fermi velocity for FS s, $\eta_{ss'} = +1$ ($\eta_{ss'} = -1$) if the FSs s and s' are of the same (different) type, and $\mathbf{e}_\perp$ denotes the unit vector perpendicular to $\mathbf{v}_{s,\mathbf{k}}$ in the plane spanned by $\mathbf{v}_{s,\mathbf{k}}$ and $\mathbf{v}_{s',\mathbf{k}'}$. Since $W_a(\theta)$ is an even function of θ, the term proportional to $\sin\theta$ averages to zero. Using the definition Eq. (3) and the assumption of elastic scattering, the term proportional to $\cos\theta$ can be written in terms of $g_{s,\mathbf{k}}$.

Factoring out $g_{s,\mathbf{k}}$, we obtain

$$e\mathbf{E} \cdot \mathbf{v}_{s,\mathbf{k}}[-f_0'(\varepsilon_{s,\mathbf{k}})] = g_{s,\mathbf{k}} \sum_{s'} N_{s'} \bigg\langle [\delta_{s'\bar{s}} W_a(\theta) + \delta_{s's} W_i]$$
$$\times \left(1 - \eta_{ss'} \frac{\tau_{s'} v_{F,s'}}{\tau_s v_{F,s}} \cos\theta \right) \bigg\rangle_\theta. \qquad (6)$$

Together with Eq. (3), this implies

$$\frac{1}{\tau_s} = N_s W_i + N_{\bar{s}} \langle W_a(\theta) \rangle_\theta - \eta_{s\bar{s}} N_{\bar{s}} \frac{\tau_{\bar{s}} v_{F,\bar{s}}}{\tau_s v_{F,s}} \langle W_a(\theta) \cos\theta \rangle_\theta. \qquad (7)$$

It is useful to define the *anisotropy parameter*

$$\epsilon \equiv 1 + \eta_{12} \frac{\langle W_a(\theta) \cos\theta \rangle_\theta}{\langle W_a(\theta) \rangle_\theta} \qquad (8)$$

as a measure of the anisotropy of $W_a(\theta)$. The limit $\epsilon = 0$ ($\epsilon = 2$) corresponds to $W_a(\theta)$ having a δ-function peak at $\theta = 0$ ($\theta = \pi$) for the e-h case and vice versa for the e-e or h-h case. $\epsilon = 1$ always corresponds to $\langle W_a(\theta) \cos\theta \rangle_\theta = 0$, which includes the case of isotropic interband scattering. Figure 1(b) illustrates the connection between ϵ and the anisotropic scattering rate for the case of a single maximum. We focus on the situation in which the maximum is at $\theta = 0$. Although our results hold for a general even function $W_a(\theta)$, for the sake of clarity we confine the discussion to an anisotropic scattering rate with a single maximum at $\theta = 0$ [see Fig. 1(b)]. Such a maximum occurs naturally for the e-h case close to an excitonic instability, due to the scattering by the enhanced spin or charge fluctuations, allowing $\epsilon \in [0,1]$ to be tuned by doping or temperature. In particular, we expect that $\epsilon \to 0$ as one approaches the excitonic instability. Although there is no excitonic instability for the e-e or h-h case, $\epsilon \in [1,2]$, collective fluctuations can still be enhanced due to the proximity of nesting.

III. TRANSPORT TIMES

We first consider pure interband scattering. Solving Eq. (7) for the TTs, we obtain

$$\tau_s = \tau_{0,s} \frac{1 + \frac{1-\epsilon}{\epsilon}\left(1 - \frac{1}{\gamma_s}\right)}{2 - \epsilon}, \qquad (9)$$

where $\tau_{0,s} = N_{\bar{s}}^{-1} \langle W_a(\theta) \rangle_\theta^{-1}$ is the bare lifetime for FS s, and $\gamma_s \equiv v_{F,s} \tau_{0,s} / v_{F,\bar{s}} \tau_{0,\bar{s}} = (k_{F,s}/k_{F,\bar{s}})^{d-1}$, where d is the dimension of the system. Note that only the surface areas of the FSs matter and not their densities of states.

The TT is plotted in Fig. 2. We first focus on the e-h case, $0 \leqslant \epsilon \leqslant 1$ [cf. Fig. 1(b)]. The smaller FS has a negative TT for

$$\epsilon < \epsilon^* \equiv 1 - \gamma_<, \qquad (10)$$

where $\gamma_< = \min \gamma_s \leqslant 1$. In the anisotropic limit, $\epsilon \to 0$, the TT of the smaller (larger) FS diverges to negative (positive) values, while their ratio remains finite and negative, $(\tau_s/\tau_{0,s})/(\tau_{\bar{s}}/\tau_{0,\bar{s}}) \to -\gamma_{\bar{s}} = -1/\gamma_s$. This can be understood as follows. For $\epsilon \to 0$, the scattering rate $W_a(\theta)$ becomes a δ function and, therefore, a particle in the state $s,\mathbf{k}$ can only scatter to the state $\bar{s},\bar{\mathbf{k}}$, where $\bar{\mathbf{k}}$ is determined by $\varepsilon_{\bar{s},\bar{\mathbf{k}}} = \varepsilon_{s,\mathbf{k}}$ and $\theta_{\mathbf{k},\bar{\mathbf{k}}} = 0$ [see Fig. 1(a)]. Thus the system decouples into pairs
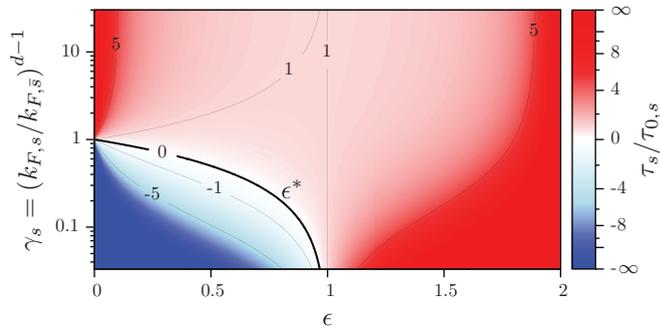
FIG. 2. (Color online) Transport time τ_s in units of the bare lifetime $\tau_{0,s}$ at FS s as a function of the anisotropy parameter ϵ and $\gamma_s = (k_{F,s}/k_{F,\bar{s}})^{d-1}$. The corresponding plot of $\tau_{\bar{s}}/\tau_{0,\bar{s}}$ would be the mirror image with respect to $\gamma_s = 1$.

of states, $s, \mathbf{k}$ and $\bar{s}, \bar{\mathbf{k}}$, thereby becoming nonergodic. The joint particle density of these two states, $F_{s,\mathbf{k}} \equiv N_s f_{s,\mathbf{k}} + N_{\bar{s}} f_{\bar{s},\bar{\mathbf{k}}}$, cannot change due to scattering and for the e-h case considered here evolves in time according to

$$\frac{dF_{s,\mathbf{k}}}{dt} = eN_s \mathbf{E} \cdot \mathbf{v}_{s,\mathbf{k}}[-f_0'(\varepsilon_{s,\mathbf{k}})]\left(1 - \frac{1}{\gamma_s}\right). \quad (11)$$

A steady state is established only for the special case of perfectly matched FSs, $\gamma_s = 1$, leading to finite TTs. Equation (9) shows that they approach the limit $\tau_s = \tau_{0,s}/2$. For $\gamma_s \neq 1$, however, the joint particle density $F_{s,\mathbf{k}}$ accelerates freely so that the TTs diverge. While this leads to diverging individual occupations $f_{s,\mathbf{k}}$, the difference $f_{s,\mathbf{k}} - f_{\bar{s},\bar{\mathbf{k}}} = g_{s,\mathbf{k}} - g_{\bar{s},\bar{\mathbf{k}}}$ approaches the finite value $\tau_{0,s} e\mathbf{E} \cdot \mathbf{v}_{s,\mathbf{k}}[-f_0'(\varepsilon_{s,\mathbf{k}})]$, which can be obtained from Eq. (1) by considering δ scattering.

For small $\epsilon > 0$, the scattering between $s, \mathbf{k}$ and $\bar{s}, \bar{\mathbf{k}}$ still dominates and scattering to other states can be treated as a weak perturbation. For the uncompensated case $\gamma_s \neq 1$, this additional scattering leads to weak relaxation of $F_{s,\mathbf{k}}$ and thus stabilizes a steady state. Still, the difference $f_{s,\mathbf{k}} - f_{\bar{s},\bar{\mathbf{k}}}$ relaxes much more rapidly than the individual occupations, so that $f_{s,\mathbf{k}} \approx f_{\bar{s},\bar{\mathbf{k}}}$ in the steady state. The occupation numbers on the same side of the two FSs are both either enhanced or reduced in comparison to the equilibrium state. In the e-h case, the electrons at these points have opposite velocities so that the electrons on one of the FSs have to drift in the "wrong" direction. As Fig. 2 shows, the direction of the drift and thus the signs of the TTs are set by the majority carriers.

On the other hand, for weak anisotropy, $\epsilon \approx 1$, Fig. 2 shows that $\tau_s/\tau_{0,s}$ decreases with decreasing ϵ regardless of the FS sizes. Increasing anisotropy favors small-θ scattering. For the e-h case, this enhances backscattering since the velocities $\mathbf{v}_{s,\mathbf{k}}$ and $\mathbf{v}_{\bar{s},\bar{\mathbf{k}}}$ are opposite and is therefore more efficient in relaxing the current. The enhanced backscattering is effective for all γ_s, including the compensated case of $\gamma_s = 1$. At this special value, it is not balanced by the previously discussed mechanism based on anisotropic scattering so that the TTs remain finite down to $\epsilon = 0$.

In the e-e or h-h case, the carriers from both FSs always drift in the same direction, as expected. The TTs increase monotonically with ϵ and diverge in the extreme anisotropic limit $\epsilon \to 2$. The increasing anisotropy favors small-θ scattering, which for the e-e or h-h case corresponds to forward

scattering, and is thus increasingly inefficient at relaxing the current.

We finally turn to the consequences of additional isotropic intraband scattering. If we include W_i in Eq. (2), the TTs become

$$\tau_s = \tau_{0,s} \frac{1 - \frac{1}{\gamma_s}\frac{1-\epsilon}{1+x_{\bar{s}}}}{1 - \frac{1-\epsilon}{1+x_s}\frac{1-\epsilon}{1+x_{\bar{s}}}}, \quad (12)$$

where the bare lifetimes now consist of intra- and interband contributions,

$$\frac{1}{\tau_{0,s}} = \frac{1}{\tau_{0,s}^{(a)}} + \frac{1}{\tau_{0,s}^{(i)}} \equiv N_{\bar{s}}\langle W_a(\theta)\rangle_\theta + N_s W_i, \quad (13)$$

and $x_s \equiv \tau_{0,s}^{(a)}/\tau_{0,s}^{(i)}$ is the ratio of the lifetimes due to inter- and intraband scattering. If we assume equal densities of states at the two FSs for simplicity we recover the previous expression Eq. (9) for the TTs with a renormalized anisotropy parameter:

$$\epsilon \to \frac{\epsilon + x}{1 + x}, \quad (14)$$

where $x = W_i/\langle W_a(\theta)\rangle_\theta$. Thus in this case the only effect of isotropic intraband scattering is to reduce the range of the anisotropy parameter to $x/(1 + x) \leqslant \epsilon \leqslant 2 - x/(1 + x)$. Note that negative TTs still occur provided that $x < 1/\gamma_< - 1$. Since the inclusion of isotropic intraband scattering essentially leads to a renormalization of the anisotropy parameter, we ignore intraband scattering in the following discussion of the transport coefficients.

IV. TRANSPORT COEFFICIENTS

A. Resistivity

The resistivity can be obtained from the TTs τ_s.[1] We present the resistivity relative to its isotropic limit, $\rho_0 \equiv \rho|_{\epsilon=1}$, which coincides with the result one would obtain by approximating the TTs by bare lifetimes. We obtain

$$\frac{\rho}{\rho_0} = \frac{v_{F,1}k_{F,1}^{d-1}\tau_{0,1} + v_{F,2}k_{F,2}^{d-1}\tau_{0,2}}{v_{F,1}k_{F,1}^{d-1}\tau_1 + v_{F,2}k_{F,2}^{d-1}\tau_2}$$

$$= \frac{2 - \epsilon}{1 + \frac{1-\epsilon}{\epsilon}\left(1 - \frac{2}{\gamma_1 + \gamma_2}\right)}. \quad (15)$$

The ratio ρ/ρ_0 is plotted in Fig. 3. The figure shows that the anisotropy has a large effect on the resistivity, especially in the e-h case. Although minority carriers give a negative contribution to the current for $\epsilon < \epsilon^*$, the total current in the direction of $\mathbf{E}$ is always positive. In the uncompensated case ($\gamma_s \neq 1$) the competition between the two anisotropy effects, the usual enhancement of the resistivity due to backscattering and the reduction due to anisotropic scattering, causes a maximum of ρ/ρ_0 as a function of ϵ at $\epsilon = \epsilon^*$.

Consistent with previous investigations[17] we find that in compensated e-h systems ρ/ρ_0 exhibits an enhancement up to a factor of 2 due to the usual backscattering. In uncompensated e-h systems, however, anisotropy of the scattering causes a strong reduction of the resistivity below $\epsilon = \epsilon^*$, which occurs already at weak anisotropy, if the mismatch between the FS radii is large.
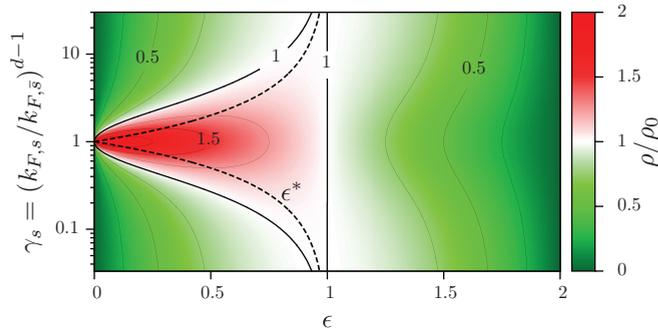
FIG. 3. (Color online) Resistivity in terms of its isotropic limit, $\rho_0 \equiv \rho|_{\epsilon=1}$, as a function of ϵ and $\gamma_s = (k_{F,s}/k_{F,\bar{s}})^{d-1}$. At $\epsilon = \epsilon^*$ (dashed curve), the TT of the minority carriers changes sign and the resistivity has a maximum as a function of ϵ.

B. Hall coefficient

The Hall coefficient of a two-band system with isotropic dispersion obeys[1]

$$R_H = \pm \frac{1}{ec} \frac{n_s \mu_s^2 + \eta_{s\bar{s}} n_{\bar{s}} \mu_{\bar{s}}^2}{(n_s \mu_s + n_{\bar{s}} \mu_{\bar{s}})^2}, \qquad (16)$$

where $\mu_s = e\tau_s v_{F,s}/k_{F,s}$ and $n_s \propto k_{F,s}^d$ are the mobility and particle number of FS s, respectively, and the upper (lower) overall sign pertains to a holelike (electronlike) FS s. With Eq. (9) we obtain

$$\frac{R_H}{R_{H,s}} = \frac{1 + \eta_{12} \gamma_s^{\frac{4-3d}{d-1}} \left[\frac{1-\gamma_s(1-\epsilon)}{1-\gamma_s^{-1}(1-\epsilon)} \right]^2}{\left[1 + \gamma_s^{-2} \frac{1-\gamma_s(1-\epsilon)}{1-\gamma_s^{-1}(1-\epsilon)} \right]^2}, \qquad (17)$$

where $R_{H,s} \propto 1/n_s$ is the Hall coefficient of FS s. In the e-h case, the electrons and holes contribute with different signs to the Hall coefficient, irrespective of the signs of the TTs. The ratio $R_H/R_{H,s}$ is plotted for the 2D and 3D cases in Fig. 4. The figure shows that $R_H/R_{H,s}$ is strongly affected by the anisotropy, implying that approximating the TT by the lifetime[15] is not sufficient. In particular, we find a maximum at

$$\epsilon^{**} \equiv \frac{(\gamma_s - 1)\left(1 - \gamma_s^{-\frac{1}{d-1}}\right)}{\gamma_s^{-\frac{1}{d-1}} + \gamma_s}, \qquad (18)$$

which corresponds to equal magnitude but opposite sign of the electron and hole mobilities, $\mu_e = -\mu_h$. At the maximum the Hall coefficient assumes the value $R_H/R_{H,s} = 1/[1 - \gamma_s^{-d/(d-1)}]$, which diverges for $\gamma_s \to 1$ so that for nearly compensated e-h systems anisotropic scattering can cause a huge enhancement of the Hall effect in agreement with Fanfarillo *et al.*[17] Going beyond Ref. 17, we predict that an extremum in the Hall coefficient should be observed when the anisotropy parameter ϵ is tuned through the value ϵ^{**}. According to Eq. (18) and Fig. 4, the anisotropy required to reach the extremum decreases (ϵ^{**} increases) for a larger mismatch between the FS radii. We speculate that this is the reason why among the pnictides LiFeAs and LiFeP, which have rather poor nesting, show the most pronounced extremum in the Hall coefficient as a function of temperature.[20,21] It is remarkable that also in 122 pnictides an extremum in the
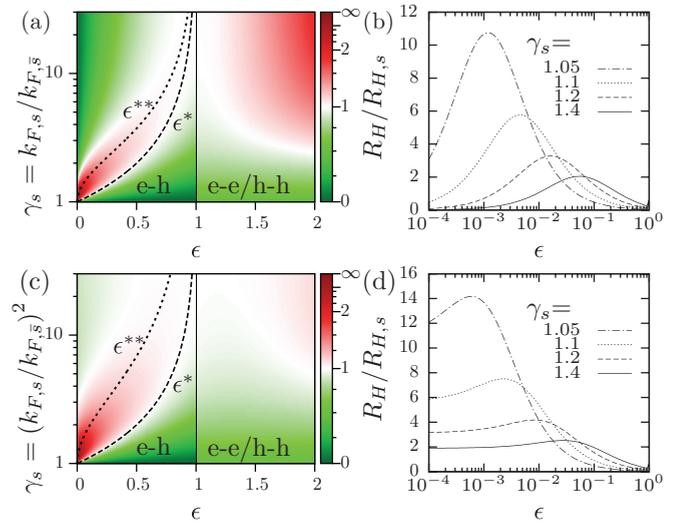
FIG. 4. (Color online) (a) Hall coefficient R_H for a 2D system as a function of ϵ and γ_s, in units of the Hall coefficient $R_{H,s}$ of FS s. (b) The same quantity as a function of ϵ on a logarithmic scale for various γ_s. (c), (d) The same as in panels (a), (b) for a 3D system. We only plot R_H in terms of $R_{H,s}$ for the larger FS ($\gamma_s \geqslant 1$); the result in terms of the smaller FS is easily obtained from Eq. (17). Note that the limit $\epsilon \to 1$ in Eq. (17) is different for the e-h and e-e or h-h cases. The characteristic anisotropy level ϵ^* where the TT of the minority carriers changes sign is indicated by a dashed line. The dotted line marked by ϵ^{**} indicates the maximum of $R_H/R_{H,s}$ as a function of ϵ.

Hall coefficient is observed for sufficiently strongly doped systems.[22]

C. Magnetoresistance

The magnetoresistance coefficient

$$\Delta\rho \equiv \frac{\rho(B) - \rho(0)}{\rho(0)B^2} \qquad (19)$$

is obtained from the standard expression[1]

$$\Delta\rho = \frac{n_1 \mu_1 n_2 \mu_2}{(n_1 \mu_1 + n_2 \mu_2)^2} \left(\frac{\mu_s}{c} - \eta_{s\bar{s}} \frac{\mu_{\bar{s}}}{c} \right)^2, \qquad (20)$$

to leading order in the magnetic field **B**. In terms of the TTs we find

$$\frac{\Delta\rho}{(\mu_{0,s}/c)^2} = \frac{\frac{\tau_1}{\tau_{0,1}} \frac{\tau_2}{\tau_{0,2}}}{\left(\frac{\tau_1}{\tau_{0,1}} \gamma_1 + \frac{\tau_2}{\tau_{0,2}} \gamma_2 \right)^2} \left(\frac{\tau_s}{\tau_{0,s}} - \eta_{12} \gamma_s^{\frac{2-d}{d-1}} \frac{\tau_{\bar{s}}}{\tau_{0,\bar{s}}} \right)^2, \qquad (21)$$

where $\mu_{0,s} = e\tau_{0,s} v_{F,s}/k_{F,s}$ is the bare mobility for FS s. Results are plotted in Fig. 5. The magnetoresistance is negative for $\epsilon < \epsilon^*$, where one TT becomes negative. Figure 6 illustrates the connection between negative TT and negative magnetoresistance. If the TT of the minority carriers is negative (positive), the current contributions $\mathbf{j}_<$ and $\mathbf{j}_>$ of minority and majority carriers, respectively, point in opposite directions (the same direction) for $\mathbf{B} = 0$. If a magnetic field is applied, the contributions $\mathbf{j}_<$ and $\mathbf{j}_>$ are rotated due to the Lorentz force, under the constraint that the total current in the transverse direction vanishes. However, as long as $\mathbf{j}_<$ and $\mathbf{j}_>$ are not rotated by the same angle, they are no longer parallel and their vector sum is thus *larger* (*smaller*) in absolute value than for
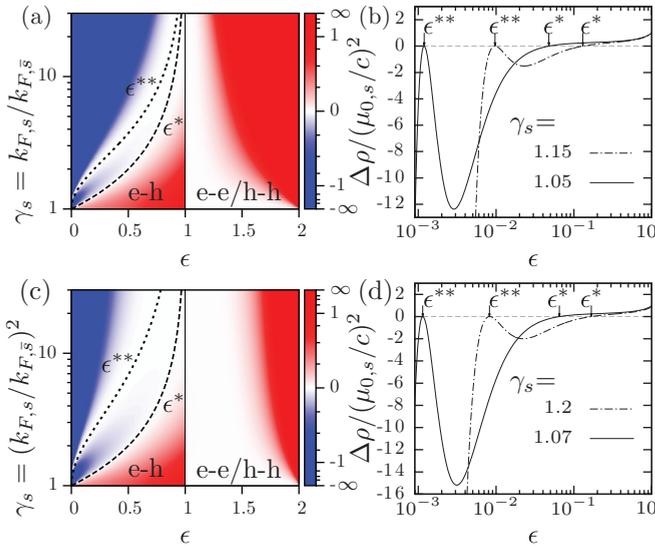
FIG. 5. (Color online) (a) Magnetoresistance coefficient for the 2D system in units of $(\mu_{0,s}/c)^2$ as a function of ϵ and γ_s and (b) as a function of ϵ for two values of γ_s. (c), (d) The same as in panels (a), (b) for a 3D system. At $\epsilon = \epsilon^*$ (dashed curve) and ϵ^{**} (dotted curve) the magnetoresistance is zero.

$\mathbf{B} = 0$. Hence, the magnetoresistance is negative (positive). A special point is $\epsilon = \epsilon^{**}$, where the two angles are equal, the total current is unchanged, and the magnetoresistance vanishes.

Since many materials of interest, such as the iron pnictides, have more than two FSs, we briefly discuss this case. In the presence of additional isotropic FSs, the magnetoresistance coefficient is determined by a sum over all pairs of FSs:

$$\Delta\rho = \frac{\frac{1}{2}\sum_{i,j=1} n_i\mu_i n_j\mu_j \left(\frac{\mu_i}{c} - \eta_{ij}\frac{\mu_j}{c}\right)^2}{\left(\sum_{i=1} n_i\mu_i\right)^2}. \qquad (22)$$

Each pair of FSs with opposite signs of the TTs gives a negative contribution to the magnetoresistance. Hence, when more than two FSs are present, the appearance of negative TTs does not necessarily lead to a negative magnetoresistance coefficient, although it can be significantly reduced. This could be relevant for the observation of an unexpectedly small magnetoresistance in certain pnictides.[13]

V. CONCLUSIONS

Anisotropic single-particle scattering between electron and hole FSs causes the transport coefficients to differ dramatically
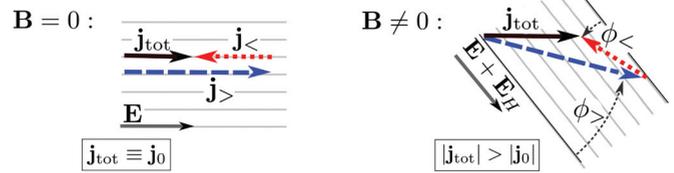
FIG. 6. (Color online) Illustration of the negative magnetoresistance below ϵ^*. The magnetic field $\mathbf{B}$ rotates the current contribution of the smaller (larger) FS, $\mathbf{j}_<$ ($\mathbf{j}_>$), by the angle $\phi_<$ ($\phi_>$), which leads to an *increase* of the total current $\mathbf{j}_{tot} = \mathbf{j}_> + \mathbf{j}_<$ if $\phi_< \neq \phi_>$. The induced Hall electric field $\mathbf{E}_H$ has no effect on the magnetoresistance but ensures that the total current points in the direction parallel to the applied electric field $\mathbf{E}$.

from the expectation based on bare lifetimes. The unexpected behavior is especially pronounced in the regime where the minority carriers have negative TTs. Here the magnetoresistance is negative, the Hall coefficient exhibits an extremum, and the resistivity decreases upon increasing the anisotropy. The degree of anisotropy required for this to occur decreases for increasing ratio between the FS areas. This effect does not depend on a particular microscopic origin for the anisotropic scattering[17] and is distinct from carrier drag due to the two-particle electron-hole interaction.[2]

Some general conclusions may be drawn. Close to perfect nesting, negative TTs are restricted to the limit of extreme scattering anisotropy and thus should only become evident in the transport just above the excitonic instability. Significant doping may therefore be required to observe the most striking effects. It is, however, encouraging that in the pnictides the magnetoresistance is rather small,[13] while the Hall coefficient is strongly enhanced close to the spin-density-wave transition,[18,19] consistent with our predictions. In contrast to what is stated in Ref. [17], we show that the Hall coefficient enhancement can be explained within the semiclassical approach. Moreover we predict that the Hall coefficient exhibits an extremum when the system is tuned through a characteristic degree of anisotropy, which becomes weaker for larger mismatch between the FS radii. This could explain the appearance of an extremum in the Hall coefficient as a function of temperature in strongly doped 122 pnictides,[18] as well as in LiFeAs and LiFeP,[20,21] which show rather poor nesting. However, the most decisive test of negative TTs resulting from anisotropic interband scattering would be the measurement of a negative magnetoresistance.

*carsten.timm@tu-dresden.de

[1] J. M. Ziman, *Principles of the Theory of Solids* (Cambridge University Press, London, 1972).

[2] T. P. McLean and E. G. S. Paige, J. Phys. Chem. Solids **16**, 220 (1960).

[3] R. A. Höpfel, J. Shah, and A. C. Gossard, Phys. Rev. Lett. **56**, 765 (1986); R. A. Höpfel, J. Shah, P. A. Wolff, and A. C. Gossard, *ibid.* **56**, 2736 (1986).

[4] H. Löhneysen, A. Rosch, M. Vojta, and P. Wölfle, Rev. Mod. Phys. **79**, 1015 (2007).

[5]B. Y.-K. Hu, Phys. Rev. Lett. **85**, 820 (2000).

[6]A. V. Chubukov, D. V. Efremov, and I. Eremin, Phys. Rev. B **78**, 134512 (2008).

[7]Q. Han, Y. Chen, and Z. D. Wang, Europhys. Lett. **82**, 37007 (2008).

[8]P. M. R. Brydon and C. Timm, Phys. Rev. B **79**, 180504(R) (2009).

[9]B. I. Halperin and T. M. Rice, Rev. Mod. Phys. **40**, 755 (1968).

[10]E. Fawcett, Rev. Mod. Phys. **60**, 209 (1988); E. Fawcett, H. L. Alberts, V. Y. Galkin, D. R. Noakes, and J. V. Yakhami, *ibid*. **66**, 25 (1994).

[11]G. Li, W. Z. Hu, D. Qian, D. Hsieh, M. Z. Hasan, E. Morosan, R. J. Cava, and N. L. Wang, Phys. Rev. Lett. **99**, 027404 (2007).

[12]H. Cercellier, C. Monney, F. Clerc, C. Battaglia, L. Despont, M. G. Garnier, H. Beck, P. Aebi, L. Patthey, H. Berger, and L. Forró, Phys. Rev. Lett. **99**, 146403 (2007).

[13]M. J. Eom, S. W. Na, C. Hoch, R. K. Kremer, and J. S. Kim, Phys. Rev. B **85**, 024536 (2012).

[14]P. Prelovšek, I. Sega, and T. Tohyama, Phys. Rev. B **80**, 014517 (2009); P. Prelovšek and I. Sega, *ibid*. **81**, 115121 (2010).

[15]A. F. Kemper, M. M. Korshunov, T. P. Devereaux, J. N. Fry, H.-P. Cheng, and P. J. Hirschfeld, Phys. Rev. B **83**, 184516 (2011).

[16]S. Onari and H. Kontani, Phys. Rev. B **85**, 134507 (2012).

[17]L. Fanfarillo, E. Cappelluti, C. Castellani, and L. Benfatto, Phys. Rev. Lett. **109**, 096402 (2012).

[18]L. Fang, H. Luo, P. Cheng, Z. Wang, Y. Jia, G. Mu, B. Shen, I. I. Mazin, L. Shan, C. Ren, and H.-H. Wen, Phys. Rev. B **80**, 140508(R) (2009).

[19]B. Shen, H. Yang, Z.-S. Wang, F. Han, B. Zeng, L. Shan, C. Ren, and H.-H. Wen, Phys. Rev. B **84**, 184512 (2011).

[20]F. Rullier-Albenque, D. Colson, A. Forget, and H. Alloul, Phys. Rev. Lett. **109**, 187005 (2012).

[21]S. Kasahara, K. Hashimoto, H. Ikeda, T. Terashima, Y. Matsuda, and T. Shibauchi, Phys. Rev. B **85**, 060503 (2012).

[22]K. Ohgushi and Y. Kiuchi, Phys. Rev. B **85**, 064522 (2012).